5-2020

The Nucleic Acid Binding Activity of Human Mitochondrial Matrix Protein Miner2

Munira Khaled

The Nucleic Acid Binding Activity of Human Mitochondrial Matrix Protein Miner2

by

Munira Khaled

Undergraduate honors thesis under the direction of

Dr. Huangen Ding

Department of Biological Sciences

Submitted to the LSU Roger Hadfield Ogden Honors College in partial fulfillment of the Upper Division Honors Program.

May, 2020

Louisiana State University
& Agricultural and Mechanical College
Baton Rouge, Louisiana

Abstract

Iron-sulfur cluster containing proteins are present in all organisms. One recently discovered group of iron-sulfur proteins containing one or two CDGSH (Cys-Asp-Gly-Ser-His) motifs has been identified in eukaryotes, bacteria, and archaea. Human mitochondria contain three different CDGSH iron-sulfur domain proteins: mitoNEET, Miner1, and Miner2. MitoNEET is the target of the diabetes drug pioglitazone and is believed to be involved in regulation of oxidative phosphorylation capacity. Furthermore, mutations of the gene encoding Miner1 lead to Wolfram syndrome. Previous studies have shown that Miner2 may regulate physiological function in the mitochondria as the binding of nitric oxide to iron-sulfur clusters do not cause cluster disruption, unlike other iron-sulfur proteins. However, little is known of the functions of Miner2. Here, we find that Miner2 interacts with double-stranded DNA (dsDNA) and thus is a DNA-binding protein. By using agarose gel electrophoresis, I was able to show that Miner2 interacts with dsDNA in a way that competitively inhibits the binding of ethidium bromide to DNA. When Miner2 binds to dsDNA, the intensity of the ethidium bromide/dsDNA complex significantly decreases. Due to this observation, we believe that Miner2 binds dsDNA and prevents ethidium bromide to bind to DNA. My data also shows that Miner2 does not bind single-stranded DNA (ssDNA), indicating that Miner2 may serve a role in protecting dsDNA from oxidative stress in the mitochondria. Alternatively, the DNA-binding activity of Miner2 may allow for Miner2 to act as a transcriptional factor to regulate gene expression in mitochondria. Further studies should be performed to fully understand the physiological effect of the DNA binding activity of Miner2 and how it relates to human health and disease.

Introduction

Iron-sulfur clusters are universally found in nature [1]. As iron-sulfur clusters can delocalize electron density between the iron atoms, the primary function of iron-sulfur clusters is to mediate electron transport [1]. Many iron-sulfur clusters are present in the mitochondria. It is believed that mitochondria contain about 20-50% of the total cellular iron and are the primary generator of iron-sulfur clusters [2]. It has been shown that iron-sulfur clusters have a wide variety of functions including acting as the substrate-binding site of enzymes, disulfide reduction and sulfur donation, and transcriptional and translational regulation of gene expression [1].

Depending on cell type, various proteins can have different iron-sulfur domains [3]. Iron-sulfur clusters involved in electron transfer contain core units of [2Fe-2S], [3Fe-4S], [4Fe-4S], or [8Fe-7S] [1] (Fig.1). Typically, cysteine coordinates to each Fe site; however, Fe can be ligated by arginine, histidine, glutamine, or serine [4]. It is possible that ligands present in each iron-sulfur cluster may modify redox potential, electron transport gating, or proton and electron transport coupling [1]. Many iron-sulfur proteins are involved in transcriptional or translational regulation of gene expression. For example, SoxR protein can sense oxidative stress via oxidation of the [2Fe-2S] cluster and stimulate the transcription of SoxS to activate the transcription of enzymes in the oxidative stress response [1]. Furthermore, iron-sulfur clusters play a key role in DNA replication and repair. One recently discovered domain is the CDGSH iron-sulfur domain (CISDs), which is present in bacteria, archaea, and eukaryotes [5]. The CDGSH iron-sulfur domain consists of one or two 17-residue CDGSH (Cys-Asp-Gly-Ser-His) motifs with a sequence of [ΦCXCXX(S/T)XXXPΦCDG(S/T/A)H], where Φ and X are a hydrophobic and any residue, respectively [5]. In this arrangement, there are three cysteine and one histidine residue present in CDGSH iron-sulfur proteins for hosting an iron-sulfur cluster [6].

Humans have three different CISD proteins present in the mitochondria; mitoNEET, mitoNEET-related protein 1 (Miner1), and mitoNEET-related protein 2 (Miner2) [5]. Originally, these proteins were annotated as zinc fingers; however, further analysis showed that there is no zinc present in the protein [7]. Instead, the proteins contain a [2Fe-2S] cluster [7]. NEET proteins are known to be involved in iron, Fe-S, and reactive oxygen homeostasis of cells; however, the principal role of each protein remains unknown. MitoNEET was the first [2Fe-2S] cluster containing protein discovered in mitochondrial outer membrane, and is encoded by gene CISD1. It was named after its subcellular location in the mitochondria (mito) and presence of the amino acid sequence Asn-Glu-Glu-Thr (NEET) [7]. Its crystal structure shows that it is an intertwined homodimer with each monomer binding to a redox active [2Fe-2S] cluster in the C-terminal cytosolic domain, which remains exposed to the cytosol [8] (Fig. 2). MitoNEET is anchored to the mitochondrial outer membrane by a transmembrane α-helix domain located in its N-terminus [9]. MitoNEET is involved in many functions and pathways. For example, deletion of mitoNEET in mice results in a decreased mitochondrial oxidative phosphorylation capacity and even phenotypic signs of Parkinson's disease [10]. Contrastingly, overexpression of mitoNEET in beta cells leads to hypoglycemia and glucose intolerance [11]. In addition, mitoNEET is highly expressed in breast cancer cells and decreased mitoNEET inhibits the proliferation of cancer cells [12]. Furthermore, mitoNEET is a target of the drug pioglitazone, a treatment for type II diabetes [13].

It has also been reported that mitoNEET [2Fe-2S] clusters can be reduced by reduced Flavin mononucleotide ($FMNH_2$) and is oxidized by oxygen or ubiquinone-2 [9]. Thus, it was determined that mitoNEET is involved in transferring electrons in the mitochondria from $FMNH_2$ to ubiquinone-2. From these results, it has been suggested that mitoNEET is involved in

regulation of oxidative phosphorylation capacity, iron homeostasis, and production of reactive oxygen species in the mitochondria [9]. However, the specific function of mitoNEET remains unknown.

Miner1 and mitoNEET share 54% of identity and 69% of similarity [14]. Similar to mitoNEET, the crystal structure of Miner1 illustrates that it is a homodimer with each monomer binding a [2Fe-2S] cluster via a 3-Cysteine-1 Histidine coordination [14]. However, Miner1 has a more open "V" shape in its Beta-Cap. This shape is due to a slight difference in the amino acid sequence present (Fig.3). Furthermore, Miner1 is membrane-bound, similar to mitoNEET. Unique to Miner1, when folded and expressed properly, Miner1 can also be located at the endoplasmic reticulum [14]. The incorrect splicing of the gene that encodes for Miner1 results in Wolfram Syndrome 2, a genetic neurological disorder [14]. This mutation results from a G to C base pair transversion in the pre-mRNA, ultimately resulting in an 75% elimination of the final protein [14]. Gene encoding Miner1 (CISD2) is located on chromosome 4, which is the chromosome associated with longevity [14]. Previous research has shown that removal of Miner1 in mice resulted in a decrease in life expectancy and general health, similarly to what is seen in individuals with Wolfram Syndrome [14].

Miner2, the newest member of the NEET family, is a soluble mitochondrial matrix protein that hosts two [2Fe-2S] clusters via two CDGSH domains [15]. This is unique to Miner2 as the other members of the NEET family contain one CDGSH domain and are lipid soluble. Furthermore, the crystal structure of Miner2 depicts that it holds two CDGSH motifs in an internal pseudodyad symmetry [5]. Miner2 has been found to be highly expressed in different types of cancers, including lung and breast. However, little information is available on the characteristics of Miner2. Previous studies have shown that nitric oxide plays a role in the

regulation of energy metabolism by interacting with iron-sulfur clusters and heme groups in proteins [16]. For example, nitric oxide works to modify [4Fe-4S] clusters in the mitochondria to block the citric acid cycle [17]. Furthermore, nitric oxide disrupts iron-sulfur clusters present in proteins due to forming a protein-bound dinitrosyl iron complex, thiolate-bridged di-ion tetranitrosyl complex, or octanitrosyl cluster [6]. However, Miner2 did not interact in a similar manner as other [2Fe-2S] iron-sulfur cluster proteins. Instead, Miner2 appears to be the first example that [2Fe-2S] clusters are able to bind to nitric oxide without any disruption of its clusters [6]. This unique binding of nitric oxide to the Miner2 [2Fe-2S] cluster may be explained by its unusual ligand arrangement of three cysteine and one histidine residues [15]. In CDGSH-type [2Fe-2S] clusters, there is a redox active iron center ligated via cysteine/histidine residues. This redox center could possibly be the site where nitric oxide binds without any disruption. Previous studies have shown that both irons in oxidized [2Fe-2S] clusters are in a ferric state. When this cluster is reduced, one of the iron atoms in the [2Fe-2S] cluster is in a ferrous state. Nitric oxide prefers to bind to the ferrous iron. Due to the favorable binding of nitric oxide to ferrous iron, it was suggested that the ferrous iron in the reduced Miner2 [2Fe-2S] clusters is the nitric oxide binding site [6]. Furthermore, it has been shown that nitric oxide-bound Miner 2 [2Fe-2S] clusters are light sensitive [18]. Upon light excitation in anaerobic conditions, nitric oxide is released from the nitric oxide-bound Miner2 and the [2Fe-2S] clusters are converted to the reduced Miner2 [2Fe-2S] clusters. This indicates that the binding of nitric oxide is a reversible process [18].

Some iron-sulfur proteins are capable of modifying gene expression by binding to DNA. The primary functions of DNA-binding proteins are to organize chromosomal DNA or to regulate DNA replication and transcription [19]. When iron-sulfur proteins bind to DNA,

activation of gene transcription is induced by recruiting RNA polymerase to bind to the promoter. Contrastingly, the binding of iron-sulfur proteins as transcriptional factors may prevent RNA polymerase from recognizing its target promoter, thus repressing transcription [20]. For example, Fumarate nitrate reductase regulator (FNR), an iron-sulfur DNA binding protein, is a homodimer that contains one O_2 sensitive $[4Fe\text{-}4S]^{2+}$ cluster per monomer that binds to specific DNA sequences [21]. By binding to DNA, FNR is capable of controlling genes involved in anaerobic respiration and metabolism [21]. Upon oxygen exposure, FNR is inactivated due to the transformation of the $[4Fe\text{-}4S]^{2+}$ cluster to a $[2Fe\text{-}2S]^{2+}$ cluster [21]. In this state, FNR acts as a transcription regulator that binds to target DNA and interacts with RNA polymerase [21]. Moreover, iron-sulfur proteins acting as regulatory proteins may affect gene expression indirectly by interfering which a downstream regulatory [20]. In this scenario, the protein senses an environmental cue, modifies the activity of the response regulator, and thus alters transcription [20]. To regulate gene expression at the post-transcriptional level, some iron-sulfur proteins may bind to mRNA transcripts and block translation, or they may promote the stability of the mRNA transcript to allow for translation to occur [20].

Miner2 was often co-purified with nucleic acids, indicating that Miner2 may have the DNA binding activity. To test our theory, we ran agarose gel electrophoresis to see if Miner2 binds to DNA. Here, we report that the human mitochondrial matrix protein Miner2 can bind double-stranded (dsDNA) DNA, but not single-stranded DNA (ssDNA). We propose that Miner2 may bind to dsDNA to regulate gene expression and protect DNA from oxidative stress.

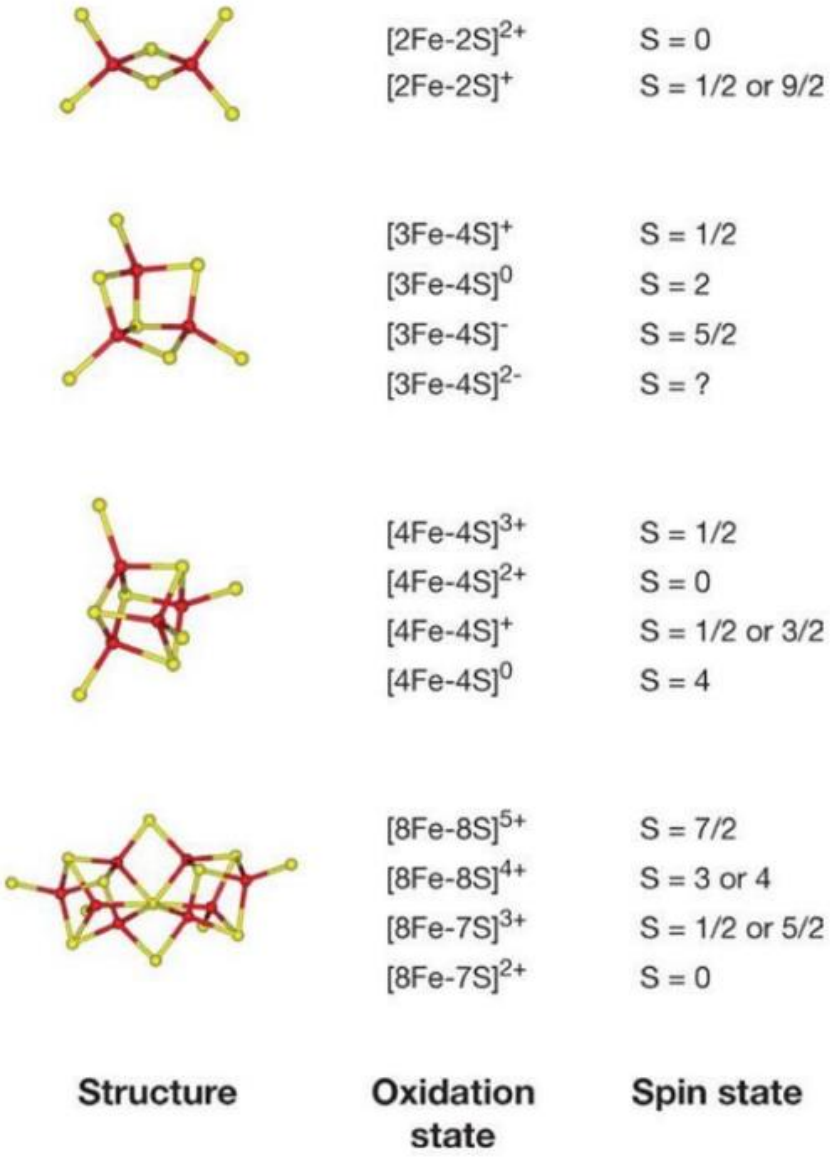

Figure 1. **Structures, core oxidation states, and spin states of crystallographically defined [Fe-S] clusters.** Iron is shown in red, and sulfur is shown in yellow. The spin state, denoted by a question mark, has yet to be determined. The [3Fe-4S] cluster has only been observed as a fragment in heterometallic [M-3Fe-4S]+ clusters (not shown) in which M is a divalent transition metal ion [1].

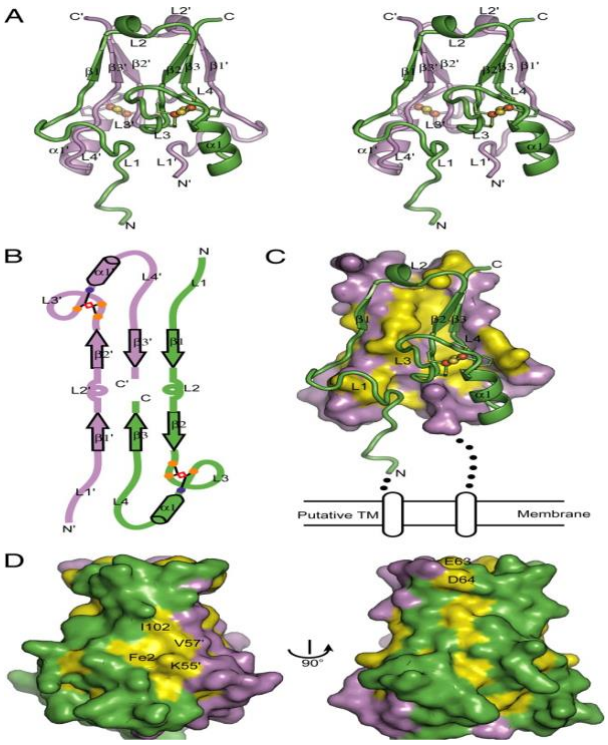

Figure 2. **Crystal structure of the soluble domain of human mitoNEET. (A) Crosseye stereoview of the ribbon representation of the structure**. The two monomer subunits are colored green and violet, respectively. The [2Fe-2S] cluster and ligand residues are represented as balls and sticks. Iron and sulfur atoms are colored orange and yellow, respectively. The secondary structure elements and N and C termini are labeled, with prime denoting the violet subunit. (B) Topology diagram of the intertwined dimer. Cysteine and histidine ligands are shown as orange and blue spots, and [2Fe-2S] clusters are shown as red rhombi. (C) The dimerization interface with the violet subunit is shown as surface representation, and the green subunit is shown as ribbons. The most highly conserved residues are colored in yellow in the violet subunit. Also shown is the relative orientation of the membrane. (D) The most highly conserved residues on the molecular surface are shown as yellow patches. [8]

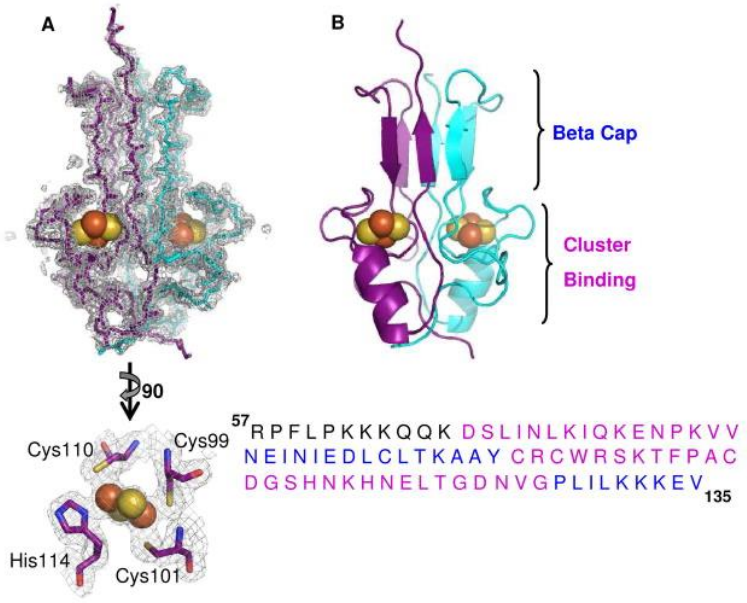

Figure 3. **Structural organization and domain topology of dimeric Miner1.(A) (Upper) The backbone tracing of homodimeric Miner1**. Protomers are colored in purple and cyan together with the observed 2Fo-Fc electron density (grey) map contoured at 1.5 σ. A 2Fe-2S cluster is present in each protomer (Fe - red spheres, S – yellow). The two protomers are related by a dyad axis along the vertical direction in the plane of the paper (see arrow). (Lower) An expanded view of one 2Fe-2S cluster (rotated ~90° counterclockwise along the dyad axis) showing the cluster and iron ligands (O colored red, N blue and C green) and the corresponding observed 2Fo-Fc electron density (grey) map contoured at 2.0σ. The amino acid ligands are indicated. (Rendered with Pymol, 39) (B) Ribbon diagram highlighting the two domains and protomer interactions within the Miner1 homodimer: a six stranded beta sandwich forms an intertwined beta cap and a larger cluster binding domain carries two 2Fe-2S clusters (one per protomer). Below is the amino acid sequence of the construct. Coded segments contributing to each domain are highlighted on the primary sequence with magenta for the beta cap and blue for the cluster binding domains. The 2Fe-2S binding cradle is located sequentially between two parts of the beta cap domains [22].

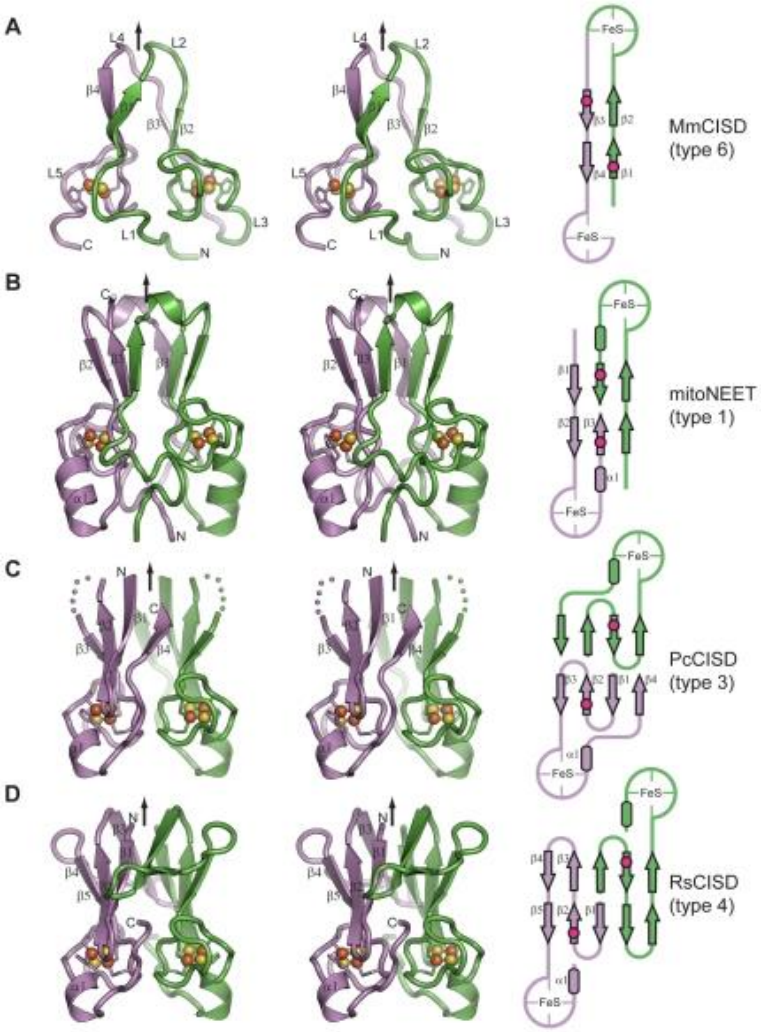

Figure 4. ***Crystal structure and topology schematic of CISDs.***(A–D) Structure and topology of type 6 MmCISD (A), type 1 mitoNEET (PDB: 2QD0 [6]) (B), type 3 PcCISD (C), and type 4 RsCISD (D). Cross-eye stereo views are shown. The two subunits or two halves for the MmCISD structure are colored in green and violet. The secondary structural elements and the N-, C-terminus are indicated for one subunit. Arrows denote the dyad axis or pseudo dyad axis for MmCISD. Red dots in schematic represent the lid-proline. [8]

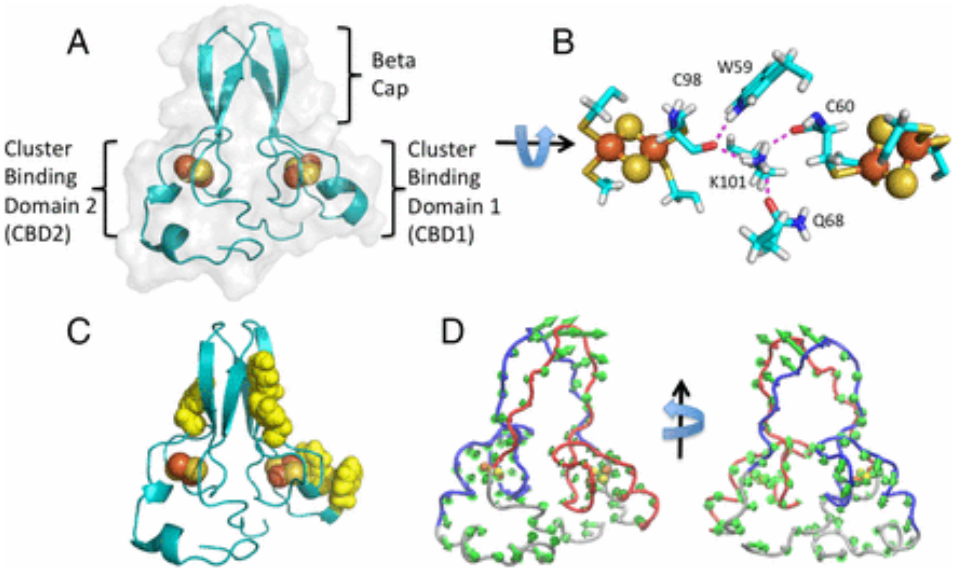

Figure 5. **Structural organization of monomeric Miner2 highlights the C2 pseudosymmetry and the asymmetrical surface.** (*A*) Miner2 contains a four-stranded beta-cap domain composed of two antiparallel hydrogen-bonded stranded sheets that dock to form the four-stranded cap domain. Each contains a structured loop and a turn of helix that contains the [2Fe-2S] cluster-coordinating ligands. However, CBD2 has additional helix and long N- and C-terminal loop extensions. (*B*) Close-up of the cluster-coordinating ligands as well as the hydrogen-bond network that connects the two clusters across the pseudosymmetrical axis. Residue numbers are indicated. (*C*) Ribbon diagram of Miner2 with surface aromatics highlighted. The clear asymmetry in the surface of Miner2 is evident in this representation. (*D*) Displacements around the average structure for the first principal component of simulated native-state dynamics, scaled 10-fold [15].

Materials and Methods

Protein Preparation

Previously, the gene encoding the human mitochondrial matrix protein Miner2 (containing residues 34-127) with the N-terminal His tag was synthesized and cloned into pET28b + plasmid for protein expression in *E. coli* cells [6]. An overnight culture of *E. coli* containing the expression plasmid were diluted 1:100 in LB (Luria-Bertani) medium and incubated at 37 °C with aeration (250 rpm) for 3 hours. Miner2 was induced at 0.60 O.D. (optical density) of by adding Isopropyl β-D-1-thiogalactopyranoside (0.5 M, 200 uL) for 14 hours at 37°C.

Following culture growth, *E. coli* cells were harvested by centrifuging for ten minutes at 4,000 rpm at 4°C. Supernatant was discarded and desalting buffer was used to resuspend and homogenize *E. coli* cell pellets. DNase was added to cell extract at a 1:100 dilution for an incubation period of thirty minutes. *E. coli* cells were then disrupted by passing the solution through French press once (pressure kept between 500-1,000 psi). Crude cell extracts were centrifuged at 15,000 rpm for one hour at 4 °C and supernatant was filtered using filter paper.

Recombinant *E. coli* Miner2 was purified using nickel-agarose column followed by a HiTrap desalting column. Protein purity was greater than 95%, as examined by electrophoresis analysis on a 15% polyacrylamide gel containing SDS (GenScript) followed by staining with Coomassie Blue. Concentration of Miner2 was measured at 280 nm using the molar coefficient of 11.9 mM^{-1} cm^{-1}. Ferredoxin was prepared and purified in the same manner as Miner2. Concentration of Ferredoxin was measured at 280 nm using the molar extinction coefficient of 73.8 mM^{-1} cm^{-1}.

Plasmid DNA Preparation

An overnight culture of *E. coli* was prepared in 5 mL LB. Plasmid was isolated from the overnight *E. coli* culture following the instructions in the ZymoPURE™ Plasmid Miniprep Kit.

Polymerase Chain Reaction

Components of polymerase chain reaction (PCR) sample: 25 μL DreamTaq Green PCR (Thermo Fischer Scientific), 20 μL dH_2O, 2 μL *E. coli* DNA template, 1 μL SoxR-1, and 1 μL SoxR-2 (OPERON).

PCR reagents were put into a thermocycler with the following settings:

Step 1 (denaturation): 95°C for 5 minutes

Step 2 (denaturation): 94°C 30 seconds

Step 3 (annealing): 62°C 30 seconds

Step 4 (based on base pair length): 72°C for 5 minutes

Step 5: Repeat steps 2-4 for 30 cycles

Step 6: 72°C for 10 minutes

Step 7: 4°C for 1 hour

Following this, PCR products were purified by using the instructions on the PureLink™ Quick Gel Extraction & PCR Purification Combo Kit (Invitrogen by Thermo Fischer Scientific). Purified PCR products was used as our source for a longer strand of dsDNA.

Single-Stranded DNA

We used SoxR-1 (OPERON) as our source of ssDNA. SoxR-1 has a nucleic acid sequence of 5’-ATAGAGCTCATGGAAAAGAAATTACCCC-3’.

Agarose Gel Preparation

Agarose gel was prepared using 50 mL 0.5x TAE buffer and 0.3 g agarose powder (MIDSCI™). Components were combined in a flask and put into a microwave for 30 seconds. Then, solution was swirled and microwaved for an additional 30 seconds to fully dissolve agarose. Following this, 0.5 μL ethidium bromide (10 mg/mL) was added and solution was swirled and poured onto gel tray with comb in place. Gel was left undisturbed for 30 minutes at room temperature until solidified.

DNA binding activity of Miner2

Different sources of DNA were used to determine whether Miner2 can interact with nucleic acids. The sample lacking any protein served as the positive control. Samples containing Ferredoxin served as the negative control because this protein does not interact with nucleic acids. The following table depicts the components used during the experiment:

Table 1. ***Sample components to determine the DNA-binding activity of human mitochondrial matrix protein Miner2.***

Miner2/ Ferredoxin Concentration (μM)	**0**	**5**	**10**	**20**
Nucleic Acid (3 $\mu g/\mu L$; μL)	1	1	1	1
Protein (μL)	0	2	4	8
Desalting Buffer (μL)	9	7	5	1

Samples were mixed with 6x non-SDS loading dye (BioLabs) and loaded into 0.6% agarose gel. Agarose gel electrophoresis ran at 80V for 20 minutes. This process was repeated independently for each different type of nucleic acid.

Effect of $MgCl_2$ on the interaction between Miner2 and DNA

To test whether $MgCl_2$ is required as a cofactor to allow for the binding of DNA to Miner2, we ran agarose gel electrophoresis with similar conditions as the increasing Miner2 concentration experiment. Here, we used 10 mM $MgCl_2$ in samples containing 20 μM Miner2, as well as 20 μM ferredoxin to serve as a negative control. The samples lacking $MgCl_2$ served as the positive control.

Components of samples:

1. 9 μL desalting buffer, 1 μL DNA
2. 1 μL desalting buffer, 1 μL DNA, 8 μL Miner2
3. 1 μL DNA, 8 μL Miner2, 1 μL 10 mM $MgCl_2$
4. 1 μL desalting buffer, 1 μL DNA, 8 μL Ferredoxin
5. 1 μL DNA, 8 μL Miner2, 1 μL 10 mM $MgCl_2$

Samples were mixed with 6x non-SDS loading dye (BioLabs) and loaded into 0.6% agarose gel. Agarose gel electrophoresis ran at 80V for 20 minutes. This process was repeated independently for each different type of DNA.

Competitive Inhibition of Ethidium Bromide

To determine if DNA is diffusing off the gel or if Miner2 is competing with ethidium bromide (EB) to bind to DNA, we decided to take UV images of the samples before and after the addition of protein.

Components of "before" samples:

1. 5 μL desalting buffer, 1 μL 3.5 ng/μL EB
2. 4 μL desalting buffer, 1 μL 3.5 ng/μL EB ,1 μL plasmid DNA

3. 4 μL desalting buffer, 1 μL 3.5 ng/μL EB, 1 μL plasmid DNA
4. 4 μL desalting buffer, 1 μL 3.5 ng/μL EB, 1 μL plasmid DNA

Components of "after" samples:

1. Addition of 4 μL desalting buffer
2. Addition of 8 μL Miner2
3. Addition of 4 μL desalting buffer
4. Addition of 8 μL Ferredoxin

"After" samples were then mixed with 6x non-SDS loading dye (BioLabs) and loaded into 0.3% agarose gel. Agarose gel electrophoresis ran at 80V for 20 minutes.

Increasing DNA Concentration

Samples with increasing DNA concentrations were run on agarose gel to determine if an overcompensation of DNA would allow for the visualizing Miner2/DNA complex on agarose gel.

Components of samples:

1. 9 μL desalting buffer, 1 μL DNA
2. 1 μL desalting buffer, 1 μL DNA, 8 μL Miner2
3. 2 μL DNA, 8 μL Miner2
4. 1 μL desalting buffer, 1 μL DNA, 8 μL Ferredoxin
5. 2 μL DNA, 8 μL Ferredoxin

Samples were mixed with 6x non-SDS loading dye (BioLabs) and loaded into 0.6% agarose gel. Agarose gel electrophoresis ran at 80V for 20 minutes. This process was used for plasmid DNA and PCR product.

Results

Human Miner2 Interacts with Double-Stranded DNA

If a complex will form between dsDNA and Miner2, band shift of DNA is expected. However, when Miner2 was incubated with plasmid DNA, the visibility of the Miner2/plasmid DNA complex in the agarose gel decreased as Miner2 concentration increased (Fig. 6). The complex intensity continued to decrease at 10 μM and no plasmid DNA band could be observed after incubation with 20 μM Miner2 (Fig. 6).

A PCR product behaved in a similar manner as plasmid DNA. The intensity of the Miner2/ DNA complex was significantly weaker than that of the positive control where Miner2 was not present. The complex intensity continued to decrease at 10 μM and no dsDNA-Miner2 complex could be observed at 20 μM Miner2 (Fig. 7).

Ferredoxin does not bind to DNA and thus there will be no protein-DNA band shift. Thus, there does appear to be an interaction between dsDNA and Miner2 (Fig.6).

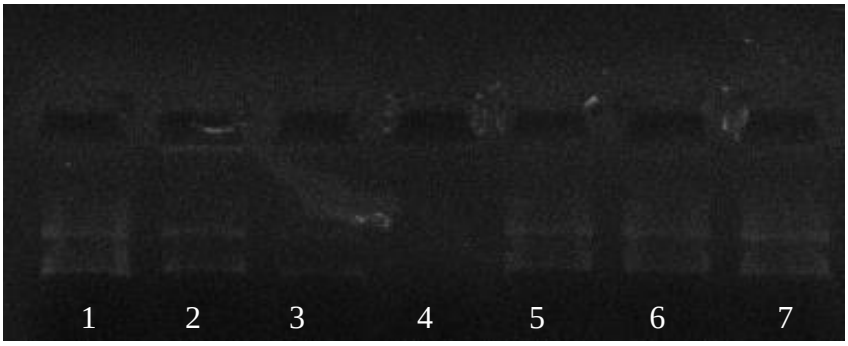

Figure 6. ***Binding of human Miner2 with plasmid DNA***. The effect of increasing Miner2 concentration on plasmid DNA binding activity. Each sample has a total volume of 10 μL. Lane one serves as the positive control of plasmid DNA. Lanes 2-4, contain Miner2 of 5 μM,10 μM, and 20 μM, respectively. Lanes 5-7, contain ferredoxin of 5 μM, 10 μM, and 20 μM, respectively. Gel electrophoresis using 0.6 % agarose gel ran for 20 minutes at 80 V.

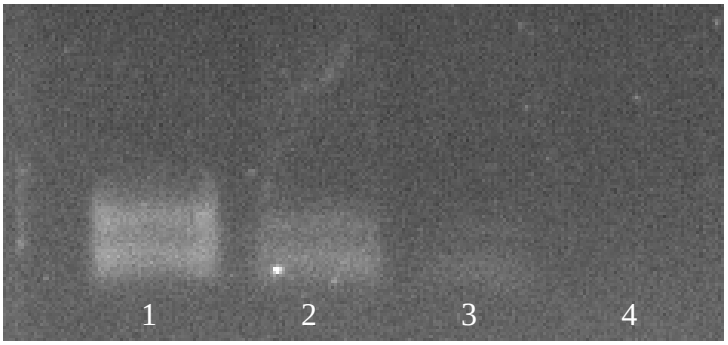

Figure 7. ***Binding of human Miner2 with PCR product.*** Each sample has a total volume of 10 μL. Lane one serves as the positive control and contains 9 μL desalting buffer and 1 μL dsDNA. Lanes 2-4, contain Miner2 of 5 μM,10 μM, and 20 μM, respectively. Gel electrophoresis using 0.6 % agarose gel ran for 20 minutes at 80 V.

Human Miner2 [2Fe-2S] Clusters Do Not Require $MgCl_2$ As a Cofactor to Bind to Double-Stranded DNA

$MgCl_2$ was chosen to use as a cofactor to determine if Miner2 requires Mg^{2+} to bind to dsDNA. After running agarose gel electrophoresis to test its effect on the visibility of the Miner2/ plasmid DNA complex, we observed that it did not increase the visibility of the complex at 20 μM Miner2 (Fig.8). Instead, the complex could not be observed and appeared as if there was no genetic material present (Fig.8).

Moreover, using PCR product as a source of dsDNA, we observed that $MgCl_2$ did not increase the visibility of the complex at 20 μM Miner2 (Fig.9). Instead, the complex could not be observed and appeared as if there was no genetic material present (Fig.9).

As expected, $MgCl_2$ did not affect the migration or visibility of the Ferredoxin/ dsDNA complexes.

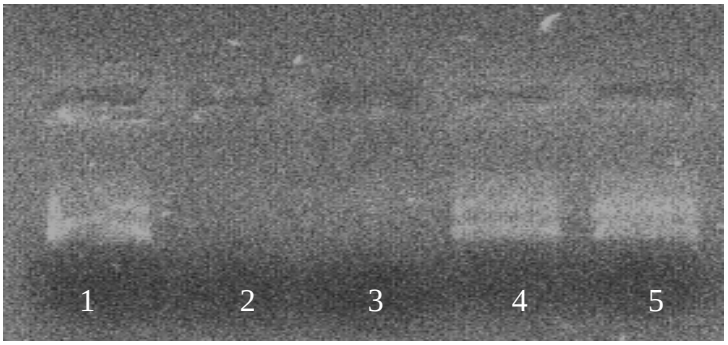

Figure 8. ***Human Miner2 does not require $MgCl_2$ to interact with Plasmid DNA***. $MgCl_2$ does not allow for the visibility of the 20 μM Miner2/plasmid DNA complex. Each sample has 1 μL Plasmid DNA (3 $\mu g/\mu L$). Lane one serves as the positive control and lacks Miner2. Lane two and three both have a Miner2 concentration of 20 μM. Lanes four and five both have a Ferredoxin concentration of 20 μM. 1 μL $MgCl_2$ is present in lanes three and five. Desalting buffer was used for volume compensation to give a total volume of 10 μL per sample. Gel electrophoresis using 0.6 % agarose gel ran for 20 minutes at 80 V.

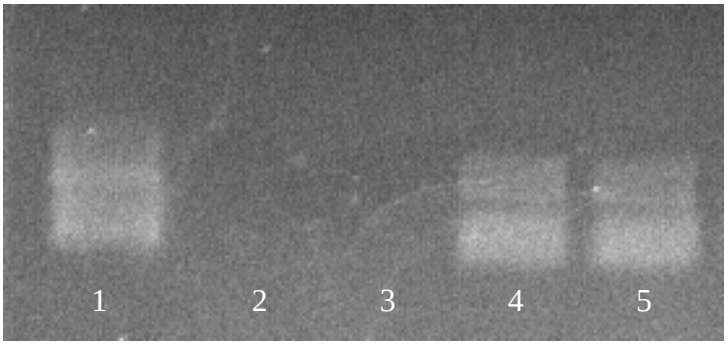

Figure 9. ***Human Miner2 does not require $MgCl_2$ to interact with PCR product.*** $MgCl_2$ does not allow for the visibility of the 20 μM Miner2/dsDNA complex. Each sample has 1 μL PCR product (3 $\mu g/\mu L$). Lane one serves as the positive control and lacks Miner2. Lane two and three both have a Miner2 concentration of 20 μM. Lanes four and five both have a Ferredoxin concentration of 20 μM and serve as the negative control. 1 μL $MgCl_2$ is present in lanes three and five. Desalting buffer was used for volume compensation to give a total volume of 10 μL per sample. Gel electrophoresis using 0.6 % agarose gel ran for 20 minutes at 80 V.

Human Miner2 competes with ethidium bromide for binding to dsDNA

After not being able to observe plasmid DNA nor PCR product at a Miner2 concentration of 20 μM, we speculated that Miner2 may compete with ethidium bromide for binding to dsDNA.

To ensure that plasmid DNA was present prior to the addition of Miner2, samples were pipetted onto saran wrap and images of the samples were taken before and after the addition of protein. Because 20 μM Miner2 could not be visualized on the gel, we decided to use this concentration to test if Miner2 was inhibiting the effect of ethidium bromide. Prior to the addition of Miner2, we confirmed that plasmid DNA was present and its intensity matched that of Ferredoxin (Fig. 10A). Once Miner2 was added to the sample, however, the intensity of the fluorescence of ethidium bromide significantly decreased (Fig. 10B). The plasmid DNA/protein complex resembled the intensity of the sample that lacked plasmid DNA. Due to this, we decided to test whether an excess of plasmid DNA could overcome this inhibition imposed by Miner2. However, after increasing the plasmid DNA concentration, we remained unable to observe any plasmid DNA fluorescence at 20 μM Miner2 (Fig. 11).

As the PCR product is much smaller in base pair size than plasmid DNA, we thought that an excess of PCR product may overcome this inhibition imposed by Miner2. However, after increasing the dsDNA concentration, we remained unable to observe any DNA fluorescence at 20 μM Miner2 (Fig. 12). This observation led us to believe that DNA was not diffusing off the gel and instead human Miner2 either inhibits the fluorescence of ethidium bromide or degrades plasmid DNA.

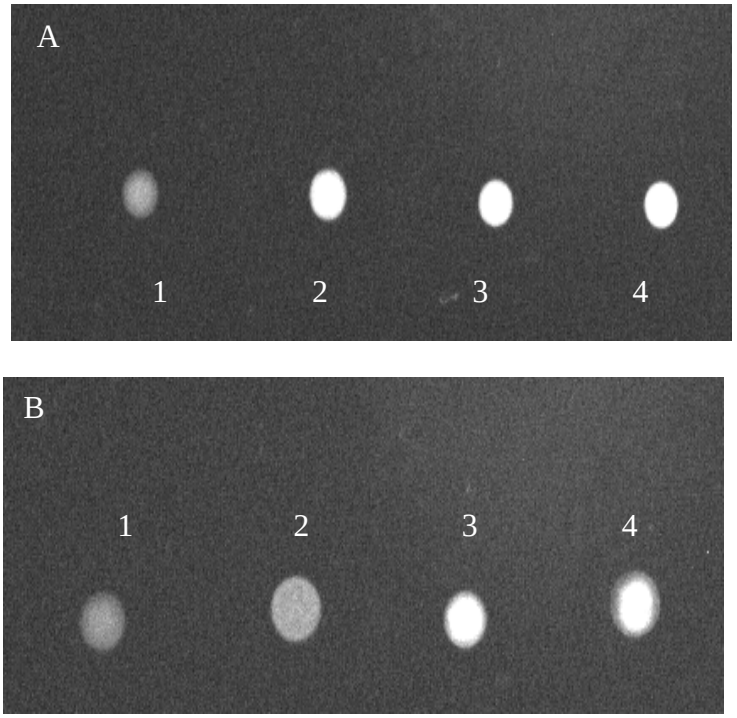

Figure 10. ***Human Miner2 competitively inhibits binding of ethidium bromide in dsDNA.*** A. *Samples prior to addition of Miner2 or Ferredoxin.* Lane one, the control of ethidium bromide without protein and plasmid DNA. Lanes 2-4, contain plasmid DNA. B. *Samples after the addition of Miner2 or Ferredoxin.* Lane 2, contains 20 μM Miner2. Lane 3, contains plasmid only. Lane 4, contains 20 μM Ferredoxin.

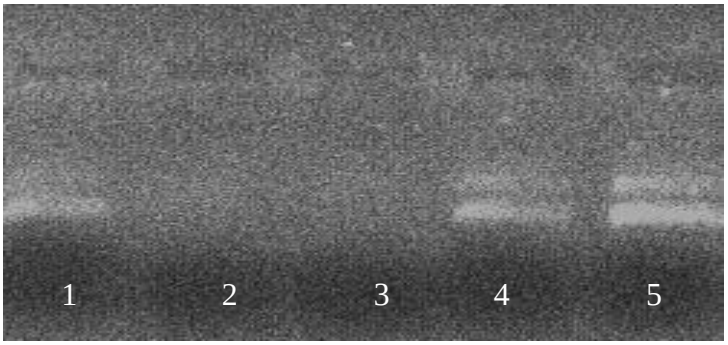

Figure 11. ***Increasing DNA concentration does not change Miner2/Plasmid DNA complex visibility***. Lane 1 is the positive control of plasmid without proteins. Lanes 2 and 3 contained Miner2 (20 μM). Lanes 4 and 5 contained Ferredoxin (20 μM). 1 μL plasmid DNA (3 μg/μL) was present in lanes 1, 2, and 4. 2 μL plasmid DNA was present in lanes 3 and 5. Gel electrophoresis using 0.6 % agarose gel ran for 20 minutes at 80 V.

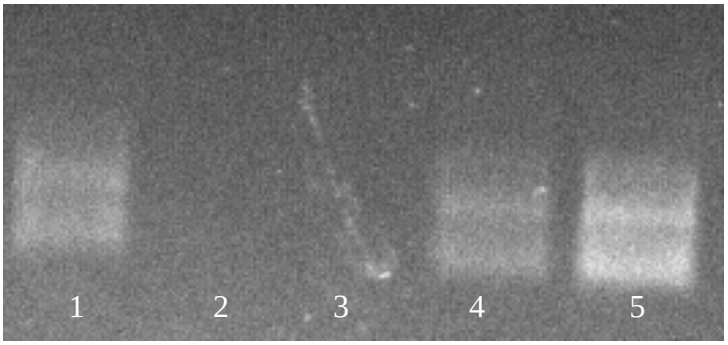

Figure 12. ***Increasing DNA concentration does not change Miner2/PCR product complex visibility***. Lane 1 is the positive control without proteins. Lanes 2 and 3 contained Miner2 (20 μM). Lanes 4 and 5 contained Ferredoxin (20 μM). 1 μL PCR product (3 μg/μL) was present in lanes 1, 2 and 4. 2 μL dsDNA was present in lanes 3 and 5. Gel electrophoresis using 0.6 % agarose gel ran for 20 minutes at 80 V.

Human Miner2 Does Not Interact with Single-Stranded DNA

Using DNA primer as a source of ssDNA, we tested to see if ssDNA behaves similarly to dsDNA in the presence of Miner2. Gel electrophoresis of samples with increasing Miner2 concentrations showed no migration of Miner2/ssDNA complexes and no changes in intensity of the complex. Unlike samples containing 20 μM Miner2 and dsDNA, the sample containing 20 μM Miner2 and ssDNA did not disappear and can be visualized on the agarose gel. Instead, all samples migrated equal lengths and resembled each other in intensity (Fig.13).

The samples that contain Miner2 behaved similarly to those containing Ferredoxin, indicating that Miner2 is not able to bind to ssDNA (Fig.13).

To test the interaction between ssDNA and Miner2, we decided to see if $MgCl_2$ as a cofactor is required to observe changes in migration distance. However, addition of $MgCl_2$ did not change the migration distance (Fig. 14).

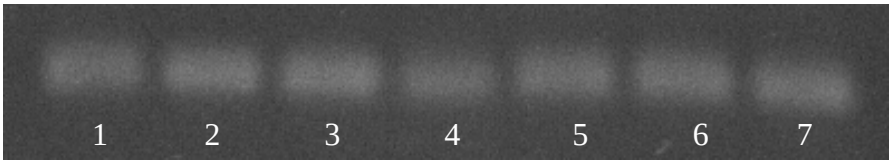

Figure 13. ***Human Miner2 has no interaction with single-stranded DNA***. The effect of increasing Miner2 concentration on single-stranded DNA binding activity. Each sample has a total volume of 10 μL and were incubated at room temperature for five minutes. Lane one serves as the positive control and contains 9 μL desalting buffer and 1 μL SoxR primer. Lane two has a Miner2 concentration of 5 μM and contains 7 μL desalting buffer ,1 μL SoxR primer, and 2 μL Miner2. Lane three has a Miner2 concentration of 10 μM and contains 5 μL desalting buffer ,1 μL SoxR primer, and 4 μL Miner2. Lane four has a Miner2 concentration of 20 μM and contains 1 μL desalting buffer ,1 μL SoxR primer, and 8 μL Miner2. Lanes five-seven serve as the negative control that do not bind to DNA and have a Ferredoxin concentration of 5, 10, and 20 $\mu M, respectively$. Gel electrophoresis using 0.6 % agarose gel ran for 20 minutes at 80 V.

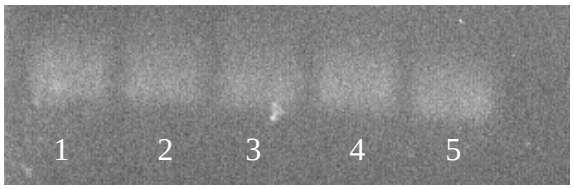

Figure 14. ***$MgCl_2$ does not allow Miner2 to bind to single-stranded DNA.*** Each sample has 1 μL dsDNA. Lane one serves as the positive control and lacks Miner2. Lane two and three both have a Miner2 concentration of 20 μM. Lanes four and five both have a Ferredoxin concentration of 20 μM and serve as the negative control. 1 μL $MgCl_2$ is present in lanes three and five. Desalting buffer was used for volume compensation to give a total volume of 10 μL per sample. Gel electrophoresis using 0.6 % agarose gel ran for 20 minutes at 80 V.

Discussion

Iron-sulfur clusters are ubiquitously found in life forms. In humans, the primary role of iron-sulfur clusters is to mediate electron transport by delocalizing electron density between two iron atoms. The majority of iron-sulfur clusters in humans are found in the mitochondria, as this is the site of electron transfer. The CDSGH iron-sulfur domain (CISDs) is a newly discovered domain that is present in bacteria, archaea, and eukaryotes. CISDs proteins bind a [2Fe-2S] cluster and are believed to be involved in iron homeostasis, iron-sulfur cluster biogenesis, and reactive oxygen homeostasis of cells.

Humans have three different CISD proteins present in the mitochondria: mitoNEET, Miner1, and Miner2. MitoNEET, the first CISD protein to be discovered, is involved in regulation of oxidative phosphorylation capacity. MitoNEET is involved in the proliferation of breast cancer and decreased mitoNEET inhibits the proliferation of cancer cells [12]. Miner1 shares similar characteristics and structure as mitoNEET, however, Miner1 has different physiological roles [14]. The incorrect splicing of CISD2, the gene that encodes for Miner1, results in Wolfram syndrome [14]. Miner2, another member of the NEET family, contains two [2Fe-2S] clusters bound by two CDGSH domains [15]. Usually, iron-sulfur clusters are disrupted in the presence of nitric oxide. However, Miner2 [2Fe-2S] clusters remain undisrupted in the presence of nitric oxide. This indicates that Miner2 may regulate mitochondrial physiological clusters by binding to nitric oxide [6]. However, the main physiological function of Miner2 remains unknown.

Many iron-sulfur proteins are capable of binding to DNA to act as regulatory proteins or protect DNA from oxidative stress. Here, we propose that Miner2 binds to DNA. Initially, we hypothesized that Miner2 will bind to DNA and create protein band shift that can be visualized

using agarose gel electrophoresis. In this case, Miner2 bound DNA will migrate slowly in agarose gel than DNA without Miner2 as the complex will be heavier. Instead, however, we observed that the intensity of the Miner2/ dsDNA complex decreases as Miner2 concentration increases. At 20 μM Miner2, the intensity of the complex disappeared as if no DNA was present. This led us to believe that Miner2 may require a cofactor to bind to DNA in a way that can be visualized under ultraviolet light. Mg^{2+} is a secondary element required as a cofactor by many enzymes and thus $MgCl_2$ was chosen as a cofactor source. However, $MgCl_2$ did not affect the visualization of the Miner2/dsDNA complexes. From this, we conclude that $MgCl_2$ has no function in the DNA interaction with Miner2. Due to this, we decided to test if Miner2 inhibits the illuminant effects of ethidium bromide. To test this, we examined the DNA-ethidium bromide samples before the addition of Miner2 to ensure that DNA is present. After the addition of Miner2, we noticed that the fluorescence intensity of the complex significantly decreased and matched the intensity of the sample that did not contain dsDNA. These results suggest that Miner2 competitively inhibits ethidium bromide binding in dsDNA. From this, we infer that Miner2 interacts with DNA in a similar manner of ethidium bromide.

Contrastingly to dsDNA, ssDNA was not found to interact with Miner2. Instead, all samples with increasing Miner2 concentrations behaved similarly to the controls. These results indicate that Miner2 is unable of binding to ssDNA.

In order to completely understand the DNA binding activity of Miner2, more tests should be performed to determine what experimental conditions are necessary for the optimal binding of Miner2 to DNA. For example, future experiments should be conducted with varying salt concentrations, pH, and temperatures to fully understand how Miner2 binds dsDNA. Further analysis should be performed to determine the physiological effect of DNA bound Miner2 in the

human mitochondria. For example, DNA-bound Miner2 may be tested in the presence of H_2O_2 to determine whether [2Fe-2S] clusters remain intact. If these clusters do remain intact, it indicates that Miner2 acts to prevent DNA damage under oxidative stress. Furthermore, tests may be conducted to see if Miner2 can recruit RNA polymerase or alter gene transcription to determine if Miner2 may act as a transcription factor.

To conclude, we propose that like many other iron-sulfur proteins human mitochondrial protein Miner2 is a DNA-binding protein. Further studies are needed to better illustrate the physiological significance of the DNA-binding activity of Miner2 in human health and diseases. Possible significances may be that DNA-binding Miner2 may help prevent DNA damage due to oxidative stress, or Miner2 may act to regulate gene expression in mitochondria by controlling transcriptional and post-transcriptional processes.

Acknowledgements

I would like to thank Dr. Huangen Ding for being my mentor and guiding me through this process. With his help, I was able to increase my knowledge on research techniques tremendously and grew as an undergraduate research. I would also like to thank Chelsea Fontenot and Homrya Tasnim for directly helping me with the techniques needed to complete my project and Lubna Qutob for helping me with the protein preparation and purification.

References

1. Johnson, D.C., et al., *STRUCTURE, FUNCTION, AND FORMATION OF BIOLOGICAL IRON-SULFUR CLUSTERS.* Annual Review of Biochemistry, 2005. **74**(1): p. 247-281.
2. Ward, D.M. and S.M. Cloonan, *Mitochondrial Iron in Human Health and Disease.* Annual Review of Physiology, 2019. **81**(1): p. 453-482.
3. Meyer, J., *Iron–sulfur protein folds, iron–sulfur chemistry, and evolution.* JBIC Journal of Biological Inorganic Chemistry, 2008. **13**(2): p. 157-170.
4. Orme-Johnson, W.H., *Iron-Sulfur Proteins: Structure and Function.* Annual Review of Biochemistry, 1973. **42**(1): p. 159-204.
5. Lin, J., et al., *Structure and Molecular Evolution of CDGSH Iron-Sulfur Domains.* PLOS ONE, 2011. **6**(9): p. e24790.
6. Cheng, Z., et al., *Binding of Nitric Oxide in CDGSH-type [2Fe-2S] Clusters of the Human Mitochondrial Protein Miner2.* Journal of Biological Chemistry, 2017. **292**(8): p. 3146-3153.
7. Paddock, M.L., et al., *MitoNEET is a uniquely folded 2Fe–2S outer mitochondrial membrane protein stabilized by pioglitazone.* Proceedings of the National Academy of Sciences, 2007. **104**(36): p. 14342-14347.
8. Lin, J., et al., *Crystal structure of human mitoNEET reveals distinct groups of iron–sulfur proteins.* Proceedings of the National Academy of Sciences, 2007. **104**(37): p. 14640-14645.
9. Li, X., et al., *Electron transfer kinetics of the mitochondrial outer membrane protein mitoNEET.* Free Radical Biology and Medicine, 2018. **121**: p. 98-104.
10. Wiley, S.E., et al., *MitoNEET is an iron-containing outer mitochondrial membrane protein that regulates oxidative capacity.* Proceedings of the National Academy of Sciences, 2007. **104**(13): p. 5318-5323.
11. Kusminski, C.M., et al., *MitoNEET-Parkin Effects in Pancreatic α- and β-Cells, Cellular Survival, and Intrainsular Cross Talk.* Diabetes, 2016. **65**(6): p. 1534-1555.
12. Sohn, Y.-S., et al., *NAF-1 and mitoNEET are central to human breast cancer proliferation by maintaining mitochondrial homeostasis and promoting tumor growth.* Proceedings of the National Academy of Sciences, 2013. **110**(36): p. 14676-14681.
13. Bieganski, R.M. and M.L. Yarmush, *Novel ligands that target the mitochondrial membrane protein mitoNEET.* Journal of molecular graphics & modelling, 2011. **29**(7): p. 965-973.
14. Karmi, O., et al., *The unique fold and lability of the [2Fe-2S] clusters of NEET proteins mediate their key functions in health and disease.* JBIC Journal of Biological Inorganic Chemistry, 2018. **23**(4): p. 599-612.
15. Lipper, C.H., et al., *Structure of the human monomeric NEET protein MiNT and its role in regulating iron and reactive oxygen species in cancer cells.* Proceedings of the National Academy of Sciences, 2018. **115**(2): p. 272-277.
16. Brown, G.C., *Nitric oxide and mitochondria.* Frontiers in Bioscience, 2007. **12**: p. 1024-1033.
17. Kennedy, M.C., W.E. Antholine, and H. Beinert, *An EPR Investigation of the Products of the Reaction of Cytosolic and Mitochondrial Aconitases with Nitric Oxide.* Journal of Biological Chemistry, 1997. **272**(33): p. 20340-20347.

18. Wang, Y., J. Lee, and H. Ding, *Light-induced release of nitric oxide from the nitric oxide-bound CDGSH-type [2Fe–2S] clusters in mitochondrial protein Miner2.* Nitric Oxide, 2019. **89**: p. 96-103.
19. Travers, A., *DNA-Binding Proteins*, in *Encyclopedia of Genetics*, S. Brenner and J.H. Miller, Editors. 2001, Academic Press: New York. p. 541-544.
20. Mettert, E.L. and P.J. Kiley, *Fe–S proteins that regulate gene expression.* Biochimica et Biophysica Acta (BBA) - Molecular Cell Research, 2015. **1853**(6): p. 1284-1293.
21. Kamps, A., et al., *Staphylococcal NreB: an O2-sensing histidine protein kinase with an O2-labile iron–sulphur cluster of the FNR type.* Molecular Microbiology, 2004. **52**(3): p. 713-723.
22. Conlan, A.R., et al., *Crystal structure of Miner1: The redox-active 2Fe-2S protein causative in Wolfram Syndrome 2.* Journal of molecular biology, 2009. **392**(1): p. 143-153.